Journal of Science and Technology in Civil Engineering NUCE 2020. 14 (2): 108–115

EFFECT OF CONFINING PRESSURE ON SHEAR RESISTANCE OF ULTRA-HIGH-PERFORMANCE FIBER REINFORCED CONCRETE

Ngo Tri Thuong[a,*]

[a]*Department of Civil Engineering, Thuyloi University, 175 Tay Son street, Dong Da district, Hanoi, Vietnam*

Article history:
Received 08/03/2020, Revised 27/03/2020, Accepted 31/03/2020

Abstract

Effect of confining pressure on the shear resistance of ultra-high-performance fiber-reinforced concrete (UHPFRCs), containing 1.5% volume content (1.5 vol.-%) of short smooth steel fiber (SS, $l = 13, d = 0.2$ mm) and long smooth steel fiber (LS, $l = 30, d = 0.3$ mm), was investigated using a new shear test method. Three levels of confining pressure were generated and maintained to the longitudinal axis of the specimen prior shear loading was applied. The test results exhibited that the shear strength of UHPFRCs was obviously sensitive to the confining pressure: the higher confining pressure produced higher shear strength. UHPFRC reinforced with 1.5 vol.-% long smooth steel fiber exhibited higher shear resistance than those reinforced with short smooth steel fiber, regardless of confining pressure levels. The confined shear strength could be expressed as an empirical function of unconfined shear strength, confining pressure, and tensile strength of UHPFRCs.

Keywords: UHPFRCs, shear resistance; confining pressure effect; smooth fiber.

https://doi.org/10.31814/stce.nuce2020-14(2)-10

1. Introduction

Ultra-high-performance fiber reinforced concrete (UHPFRCs) has been exhibited very high compressive strength, tensile strength, shear strength, strain capacity, and energy absorption capacity [1–8]. It is, therefore, expected to apply widely into the civil infrastructures to enhance their shear resistance subjected to extreme loads, such as impact and blast loads [3–6, 8, 9]. However, the application of UHPFRCs to civil infrastructures is still very limited owing to its complex characters, such as fiber reinforcement parameter dependence as well as confining pressure dependence.

Several methods have been applied to investigate the confining pressure shear dependence of normal concrete (NC) as well as fiber reinforced concrete (FRC) including push-off specimens [10–13], punch-through specimens (PTS) [14–17], and Iosipescu specimens [18, 19]). However, these methods cannot indicate the unique strain-hardening response (accompanied by the formation of multiple microcracks) of UHPFRCs under tension, owing to using the pre-crack on the specimen to govern the shear crack path. Ngo et al. [2] have proposed a new shear test method to investigate the shear resistance of UHPFRCs capable of measuring the shear-related hardening response of UHPFRCs, accompanied with multiple microcracks. This method, later, has developed by Ngo et al. [4] to investigate the confining shear dependence of UHPFRCs. However, they have just investigated with 1.5 vol.-% of medium smooth steel fiber (MS, $l/d = 19/0.2$).

*Corresponding author. *E-mail address:* trithuong@tlu.edu.vn (Thuong, N. T.)

This study aims to investigate the effect of confining pressure on the shear resistance of UHPFRCs reinforced with different types of fiber: 1.5 vol.-% of the short smooth (SS, l/d = 13/0.2) fiber and the long smooth (LS, l/d = 30/0.3) were investigated.

2. Experimental program

Fig. 1 shows an experimental program designed for investigating the effect of confining pressure on the shear resistance of UHPFRCs: six series of specimens were cast and tested. In the notation of the series, the two first letters designate the fiber types ("SS" for short smooth fiber and "LS" for long smooth fiber) while the next two characters represent the confining pressure level ("02" for 2.0 MPa confining pressure).

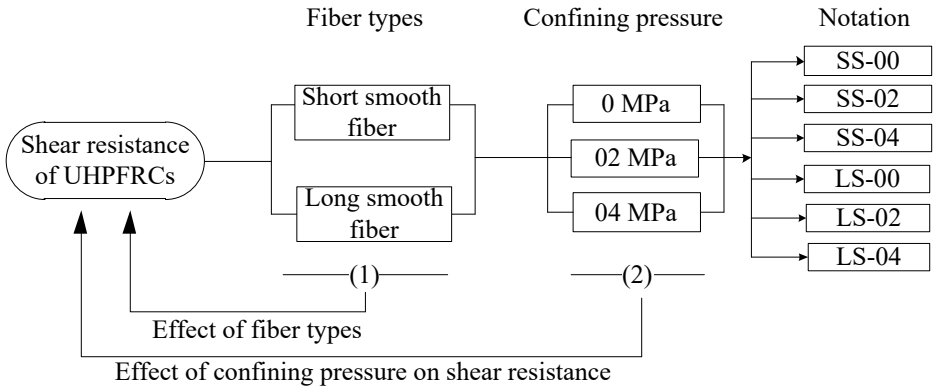

Figure 1. Experimental program

2.1. Material and specimen preparation

The composition and compressive strength of ultra-high-performance concrete (UHPC) matrix are provided in Table 1, while the properties of smooth steel fibers are listed in Table 2. The detail of mixing and curing procedure could be found in [2, 20]. A Hobart 20-L capacity type mixer with a controllable rotation speed was used to mix the UHPC mixture. Silica fume and silica sand were first dry-mix for 5 min before silica powder and cement (Type I) was added and mix about 5 min more. Water and superplasticizer were then gradually added as the dry compositions show well-distribution. After the mortar showed suitable workability and viscosity, the fiber distributed by hand and mixed about 2 min for uniform fiber distribution.

Table 1. The composition of UHPC matrix by weight ratio

Cement (Type I)	Silica fume	Silica sand	Silica powder	Super-plasticizer	Water	Compressive strength
1	0.25	1.10	0.30	0.067	0.2	180 MPa

The mixture was poured into molds with no vibration and stored in room temperature for 48 hours before demolding and curing in water at 90 ± 2°C for 3 days. All specimens were tested at the age of 28 days.

Table 2. Properties of smooth steel fibers

Fiber types, 1.5 vol.-%	Diameter, d_f (mm)	Length, l_f (mm)	Density, ρ (g/cc)	Tensile strength, σ_u (MPa)	Elastic modulus, E (GPa)
Short smooth steel fiber - SS	0.2	13	7.90	2580	200
Long smooth steel fiber - LS	0.3	30	7.90	2580	200

2.2. *Test setup and procedure*

Fig. 2 shows the shear test setup with a confining pressure frame. A high strength aluminum frame was designed to apply and maintain a compressive load along the longitudinal axis of the specimen. The shear specimen was placed into the confining pressure frame and the rotating screw at the end of the frame was tightened to generate the compressive load in the longitudinal axis of the specimen. The pre-stressed level was measured by an indicator system and a load cell installing coaxial with the longitudinal axis of the specimen. Three levels (0, 2, and 4 MPa) of pre-stressed were used in this study. Details of the test methods and testing procedures can be found elsewhere [21].

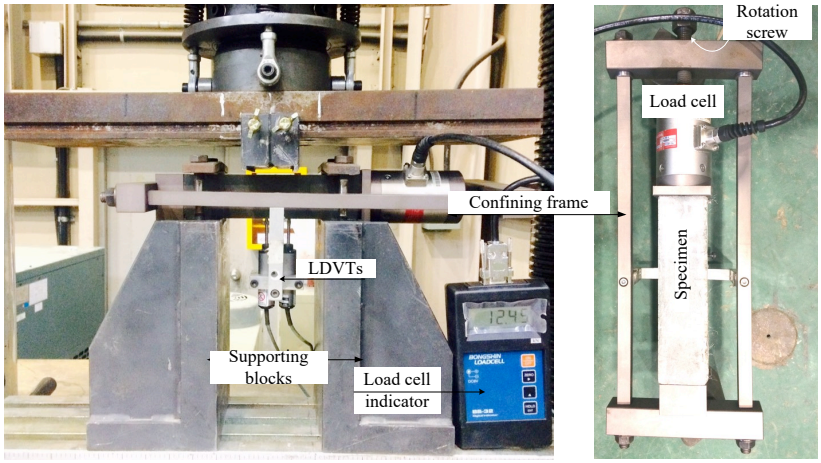

Figure 2. Shear test setup with confining frame

The shear test setup was installed in a universal testing machine (UTM). The shear load was applied to the specimen by upwards movement of the lower element of the UTM at a constant speed of 1 mm/min. The applied load was measured by a load cell inside the UTM, while the vertical displacement of the middle region of the specimen was measured by two linear variable displacement transducers (LDVTs).

3. Results

Fig. 3 shows the shear stress-versus-strain curves of UHPFRCs. The shear stress (τ) was calculated using Eq. (1), while shear strain (γ) was calculated using Eq. (2):

$$\tau = \frac{P}{2bd} \tag{1}$$

$$\gamma = \frac{\delta}{a} \tag{2}$$

where b is the specimen width (mm), P is the applied load (kN), d is the depth of the specimen (mm), a is shear span (mm) and δ is the vertical displacement in the middle part of the specimen. $\tau_{\max}$ is the peak value of the shear stress-versus-strain curve; $\gamma_{\max}$ is the shear strain at $\tau_{\max}$ and Tsp is the area under shear stress-versus-strain curve up to $\tau_{\max}$. The $\tau_{\max}$, $\gamma_{\max}$, and T_{sp} were averaged and summarized in Table 3.

Table 3. Test results

Test series	Spec.	Confining pressure, σ_l (MPa)	Shear strength, $\tau_{\max}$ (MPa)	Shear strain at peak stress, $\gamma_{\max}$ (%)	Shear peak toughness, T_{sp} (MPa)
00-SS	SP1	0	18.30	0.054	0.75
	SP2	0	18.88	0.046	0.67
	SP3	0	17.88	0.055	0.66
	SP4	0	18.13	0.054	0.81
	SP5	0	17.78	0.049	0.70
	SP6	0	17.88	0.055	0.80
	Average	0	18.10	0.052	0.73
	Standard deviation		0.4	0.004	0.07
02-SS	SP1	2	23.87	0.053	1.07
	SP2	2	25.93	0.057	1.17
	SP3	2	24.34	0.053	1.04
	SP4	2	24.85	0.052	1.03
	SP5	2	25.52	0.058	1.18
	Average	2	24.90	0.055	1.10
	Standard deviation		0.8	0.003	0.07
04-SS	SP1	4	31.94	0.054	1.44
	SP2	4	30.45	0.064	1.61
	SP3	4	32.80	0.061	1.60
	SP4	4	31.09	0.060	1.53
	SP5	4	29.80	0.067	1.59
	Average	4	31.20	0.061	1.55
	Standard deviation		1.2	0.005	0.07
00-LS	SP1	0	22.19	0.067	1.06
	SP2	0	24.25	0.065	1.09
	SP3	0	23.22	0.061	0.98
	SP4	0	24.25	0.068	1.19
	SP5	0	23.58	0.062	1.01
	SP6	0	22.23	0.070	1.17
	Average	0	23.30	0.066	1.08
	Standard deviation		0.9	0.004	0.08
02-LS	SP1	2	31.84	0.072	1.54
	SP2	2	33.76	0.071	1.23
	SP3	2	31.42	0.064	1.36
	SP4	2	33.06	0.094	1.05
	SP5	2	32.50	0.066	0.91
	SP6	2	31.96	0.061	1.29
	Average	2	32.42	0.071	1.23
	Standard deviation		0.9	0.012	0.22
04-LS	SP1	4	36.20	0.088	2.35
	SP2	4	37.00	0.091	2.31
	SP3	4	35.72	0.105	1.20
	SP4	4	38.75	0.059	1.42
	SP5	4	37.27	0.085	1.27
	SP6	4	37.35	0.080	1.99
	Average	4	37.00	0.085	1.76
	Standard deviation		1.1	0.015	0.52

The typical failure of UHPFRC specimen is shown in Fig. 3(c): all specimens failed with multiple flexural-shear cracks on the front and back sides of the specimen, accompanied with two major shear cracks.

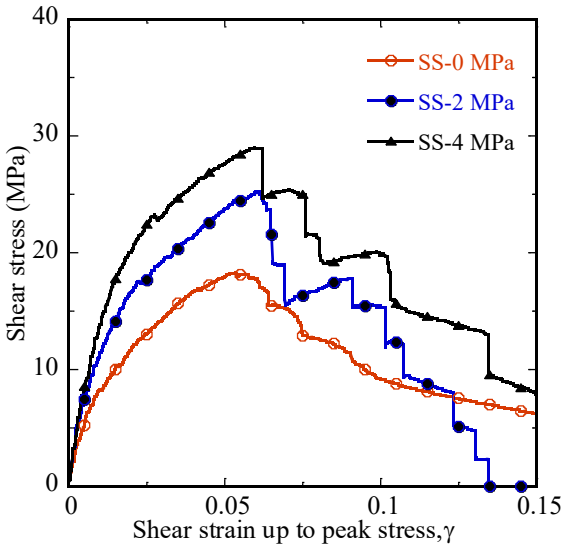

(a) UHPFRC with 1.5 vol.% SS

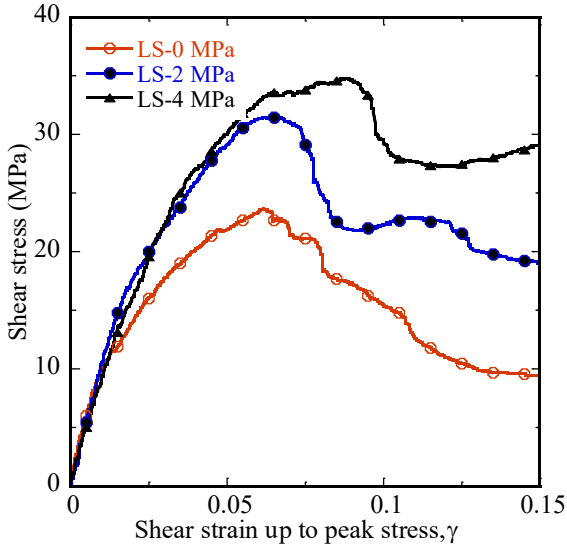

(b) UHPFRC with 1.5 vol.% LS

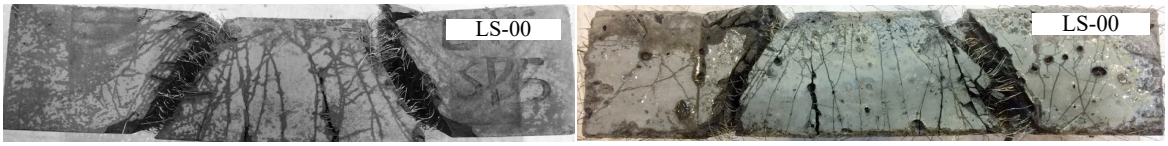

(c) Failure of shear specimens (front and back side)

Figure 3. Shear stress-versus-strain curves of UHPFRCs at different confining pressure

4. Discussions

Fig. 4 expressed the effects of confining pressure on the shear resistance of UHPFRCs. The shear strength and shear strain capacity were strongly dependent on the confining pressure level. The $\tau_{\max}$ of UHPFRC reinforced with 1.5 vol.-% SS fiber increased from 18.1 to 24.9 and 31.2 MPa as the confining pressure (σ_l) increased from 0 to 2 and 4 MPa, while those of UHPFRC reinforced with 1.5 vol.-% LS fiber are 23.3, 32.4 and 37.0 MPa. The results were well-matched with previous experimental results reported by [4, 22]. The shear strain capacity slightly increased as the confining pressure increased. The $\gamma_{\max}$ of UHPFRC containing 1.5 vol.-% SS fiber increased from 0.052 to 0.055 and 0.061 when the confining pressure increased from 0 to 2.0 and 4.0 MPa, while those values of LS fiber were 0.066, 0.071, and 0.085. Consequently, T_{sp} also increased as confining pressure increased owing to the increase of $\tau_{\max}$ and $\gamma_{\max}$, as shown in Fig. 4(c).

Among the investigated fiber reinforcement, the UHPFRC reinforced with higher fiber aspect ratio (l/d) produced higher shear resistance in terms of shear strength, shear strain capacity, and shear peak toughness, regardless the confining pressure level, as can be seen in Fig. 4. The shear resistance of UHPFRC reinforced with the long smooth steel fiber (LS, $l/d = 30/0.3 = 100$) are higher than

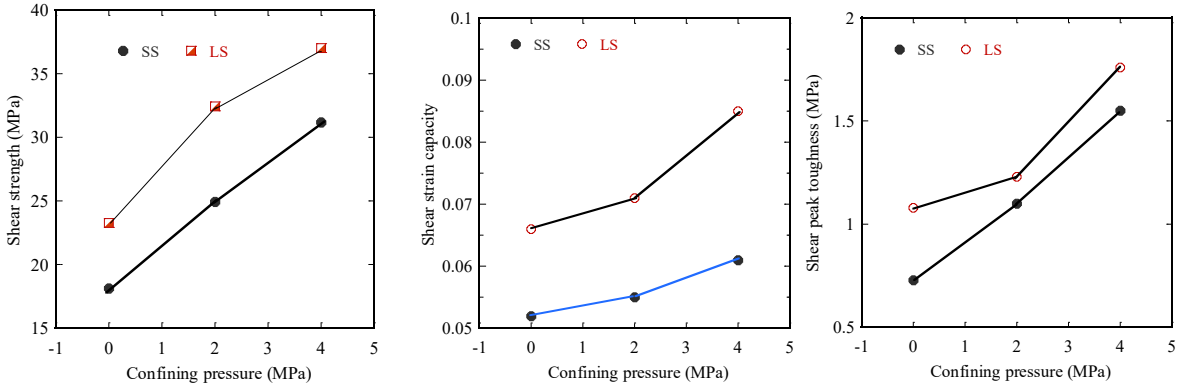

(a) Shear strength (b) Shear strain capacity (c) Shear peak toughness

Figure 4. Effect of confining pressure on the shear resistance of UHPFRCs

those of short smooth steel fiber (SS, $l/d = 13/0.2 = 65$), while those of medium smooth steel fiber (MS, $l/d = 19/0.2 = 95$) were in the middle according to Ngo et al. [23]. A similar trend was experimentally by Tran et al. [5] for tensile resistance and agree with the theoretical equation proposed by Wille et al. [24]: the resistance of UHPFRC is proportional to the aspect ratio (l/d) of fiber reinforcement.

The relation between confining shear strength of UHPFRCs and confining pressure level can be expressed by an empirical formulation based on the experimental results [4]. The shear failure in this study was governed by diagonal tensile failure along the shear plane, which was demonstrated by both theoretical and experimental analysis results [21]. Therefore, the confined shear strength (τ_{conf}) was proposed as a function of tensile strength (σ_t) and confining pressure (σ_l) by Eqs. (3) and (4) and their relationship is plotted in Fig. 5.

$$\tau_{conf} = \tau_{\max} + 1.863\sqrt{\sigma_l \sigma_t} \quad (3)$$

$$\tau_{conf} = \tau_{\max} + 1.951\sqrt{\sigma_l \sigma_t} \quad (4)$$

where $\tau_{\max}$ is the unconfined shear strength, MPa; σ_l is confining pressure, MPa; σ_t (= 10.90 in Eq. (3) and 11.10 MPa in Eq. (4)) are the post-cracking tensile strength of UHPFRC reinforced with 1.5 vol.-% the SS and LS fiber, respectively, according to Tran et al. [5].

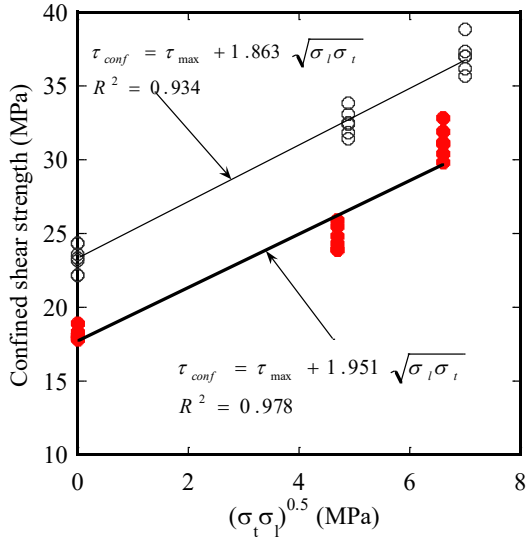

Figure 5. Proposed prediction equation for confined shear strengths of UHPFRCs

5. Conclusions

The effects of confining pressure on the shear resistance of UHPFRC were investigated using a new shear test method. The following observations and conclusions can be drawn from this study:

- The shear strength of UHPFRC was strongly dependent on the confining pressure level: the confined shear strength increased as the applied confining pressure increased.

- UHPFRC reinforced with 1.5 vol.-% long smooth steel fiber exhibited higher shear resistance than those reinforced with short smooth steel fiber, regardless of confining pressure levels.

- The confining shear strength could be predicted base on the unconfined shear strength, confining strength, and tensile strength by an empirical in this study.

Acknowledgements

This research is funded by Vietnam National Foundation for Science and Technology Development (NAFOSTED) under grant number 107.01-2019.03.

References

[1] Wille, K., Naaman, A. E., Parra-Montesinos, G. J. (2011). Ultra-High Performance Concrete with Compressive Strength Exceeding 150 MPa (22 ksi): A Simpler Way. *ACI Materials Journal*, 108(1).

[2] Ngo, T. T., Park, J. K., Pyo, S., Kim, D. J. (2017). Shear resistance of ultra-high-performance fiber-reinforced concrete. *Construction and Building Materials*, 151:246–257.

[3] Ngo, T. T., Kim, D. J. (2018). Shear stress versus strain responses of ultra-high-performance fiber-reinforced concretes at high strain rates. *International Journal of Impact Engineering*, 111:187–198.

[4] Ngo, T. T., Kim, D. J., Moon, J. H., Kim, S. W. (2018). Strain rate-dependent shear failure surfaces of ultra-high-performance fiber-reinforced concretes. *Construction and Building Materials*, 171:901–912.

[5] Tran, N. T., Tran, T. K., Kim, D. J. (2015). High rate response of ultra-high-performance fiber-reinforced concretes under direct tension. *Cement and Concrete Research*, 69:72–87.

[6] Hoan, P. T., Thuong, N. T. (2019). Shear resistance of ultra-high-performance concrete reinforced with hybrid steel fiber subjected to impact loading. *Journal of Science and Technology in Civil Engineering (STCE)-NUCE*, 13(1):12–20.

[7] Thang, N. C., Thang, N. T., Hanh, P. H., Tuan, N. V., Thanh, L. T., Lam, N. T. (2013). Research and manufacture of ultra-high-performancez concrete using silica fume and fine granulated blast furnace slag in Vietnam. *Journal of Science and Technology in Civil Engineering (STCE)-NUCE*, 7(1):83–92. (in Vietnamese).

[8] Danh, L. B., Hoa, P. D., Thang, N. C., Linh, D. D., Dung, B. T. T., Loc, B. T., Dat, D. V. Experimental research on the impact load ability of ultra-high performance concrete materials (UHPC). *Journal of Science and Technology in Civil Engineering (STCE)-NUCE*, 13(3V):12–21. (in Vietnamese).

[9] Ngo, T. T., Kim, D. J. (2018). Shear stress versus strain responses of ultra-high-performance fiber-reinforced concretes at high strain rates. *International Journal of Impact Engineering*, 111:187–198.

[10] Mattock, A. H., Hawkins, N. M. (1972). Shear transfer in reinforced concrete—Recent research. *PCI Journal*, 17(2):55–75.

[11] Valle, M., Buyukozturk, O. (1993). Behavior of fiber reinforced high-strength concrete under direct shear. *ACI Materials Journal*, 90(2):122–133.

[12] Barragan, B., Gettu, R., Agullo, L., Zerbino, R. (2006). Shear failure of steel fiber-reinforced concrete based on push-off tests. *ACI Materials Journal*, 103(4):251.

[13] Millard, S. G., Molyneaux, T. C. K., Barnett, S. J., Gao, X. (2010). Dynamic enhancement of blast-resistant ultra high performance fibre-reinforced concrete under flexural and shear loading. *International Journal of Impact Engineering*, 37(4):405–413.

[14] JSCE-SF6 (1990). *Method of test for shear strength of steel fiber reinforced concrete*. Japan Society of Civil Engineers, 67–69.

[15] Rao, G. A., Rao, A. S. (2009). Toughness indices of steel fiber reinforced concrete under mode II loading. *Materials and structures*, 42(9):1173–1184.

[16] Boulekbache, B., Hamrat, M., Chemrouk, M., Amziane, S. (2012). Influence of yield stress and compressive strength on direct shear behaviour of steel fibre-reinforced concrete. *Construction and Building Materials*, 27(1):6–14.

[17] Banthia, N., Majdzadeh, F., Wu, J., Bindiganavile, V. (2014). Fiber synergy in Hybrid Fiber Reinforced Concrete (HyFRC) in flexure and direct shear. *Cement and Concrete Composites*, 48:91–97.

[18] van Zijl, G. P. A. G. (2007). Improved mechanical performance: Shear behaviour of strain-hardening cement-based composites (SHCC). *Cement and Concrete Research*, 37(8):1241–1247.

[19] Li, V. C., Mishra, D. K., Naaman, A. E., Wight, J. K., LaFave, J. M., Wu, H.-C., Inada, Y. (1994). On the shear behavior of engineered cementitious composites. *Advanced Cement Based Materials*, 1(3): 142–149.

[20] Park, J. J., Kang, S. T., Koh, K. T., Kim, S. W. (2008). Influence of the ingredients on the compressive strength of UHPC as a fundamental study to optimize the mixing proportion. In *Proceedings of the Second International Symposium on Ultra High Performance Concrete*, 105–112.

[21] Ngo, T. T., Park, J. K., Pyo, S., Kim, D. J. (2017). Shear resistance of ultra-high-performance fiber-reinforced concrete. *Construction and Building Materials*, 151:246–257.

[22] Lukić, B., Forquin, P. (2016). Experimental characterization of the punch through shear strength of an ultra-high performance concrete. *International Journal of Impact Engineering*, 91:34–45.

[23] Ngo, T. T., Kim, D. J. (2018). Synergy in shear response of ultra-high-performance hybrid-fiber-reinforced concrete at high strain rates. *Composite Structures*, 195:276–287.

[24] Wille, K., El-Tawil, S., Naaman, A. E. (2014). Properties of strain hardening ultra high performance fiber reinforced concrete (UHP-FRC) under direct tensile loading. *Cement and Concrete Composites*, 48: 53–66.